Unraveling the Electronic Structure of Individual Photosynthetic Pigment-Protein Complexes

Oijen, Antoine M. van; Ketelaars, Martijn; Köhler, Jürgen; Aartsma, Thijs J.; Schmidt, Jan

Published in:
Science

Publication date:
1999

Newcomb, and H. E. Dregne [*Int. J. Remote Sens*. **15**, 3547 (1994)]. SOI and SST data are produced and archived by the National Oceanographic and Atmospheric Administration/Climate Prediction Center (http://www.cpc.ncep.noaa.gov/). A previous paper (*4*) proposed the use of a satellite-derived potential virus activity factor. We now use monthly NDVI data, normalized to represent departures from the 1982–95 mean, to better characterize rainfall anomalies associated with RVF activity.

14. T. M. Logan, K. J. Linthicum, F. G. Davies, Y. S. Binepal, C. R. Roberts, *J. Med. Entomol*. **28**, 293 (1991); T. M. Logan, F. G. Davies, K. J. Linthicum, T. G. Ksiazek, *Trans. R. Soc. Trop. Med. Hyg*. **86**, 202 (1992).
15. M. A. Cane, G. Eshel, R. W. Buckland, *Nature* **370**, 204 (1994).
16. S. E. Nicholson, *Int. J. Climatol*. **17**, 345 (1997); _____ and J. Kim, *ibid.*, p. 117.
17. There is a direct relation between rainfall and green vegetation growth, between green vegetation growth and the NDVI, and hence between rainfall and the NDVI. This relation applies to areas receiving precipitation of <800 mm/year. W. K. Lauenroth, in *Perspectives in Grassland Ecology*, N. French, Ed. (Springer-Verlag, New York, 1979), pp. 3–24; H. N. Le Houerou and C. H. Hoste, *J. Range Manage*. **30**, 181 (1977); A. R. Malo and S. E. Nicholson, *J. Arid Environ*. **19**, 1 (1990); S. E. Nicholson, M. L. Davenport, A. R. Malo, *Clim. Change* **17**, 209 (1990); C. J. Tucker and S. E. Nicholson, *Ambio*, in press.
18. B. N. Holben, Y. J. Kaufman, J. D. Kendall, *Int. J. Remote Sens*. **11**, 1511 (1990); E. F. Vermote and Y. J. Kaufman, *ibid*. **16**, 2317 (1995); S. O. Los, *ibid*. **14**, 1907 (1994); N. Che and J. C. Price, *Remote Sens. Environ*. **41**, 19 (1992).
19. Correlation coefficients were determined for a data series calculated by the differences between adjacent values with SPSS Trends 6.1 software (SPSS, Chicago, 1994). Nairobi NDVI anomalies were derived from average monthly composite data within 8 by 8 grid cells, each with a spatial resolution of 8 km centered close to Nairobi, Kenya. Monthly AVHRR data were derived from global area coverage data that are produced by the on-board processing of large area coverage data (1.1 km by 1.1 km) and subsequently transmitted to receiving stations in Virginia or Alaska. Composite data were formed by selecting the highest NDVI for each grid cell location from daily data for that month to minimize cloud and atmospheric contamination. NDVI data were calculated and mapped to a Hammer-Aitof projection. The highest value during a monthly period was selected to represent the monthly composite for each grid cell location.
20. AutoRegressive Integrated Moving Average (ARIMA) analysis determined by SPSS, Trends 6.1 software.
21. T. M. Logan *et al.*, *J. Am. Mosq. Control Assoc*. **6**, 736 (1990).

5 February 1999; accepted 5 May 1999

Unraveling the Electronic Structure of Individual Photosynthetic Pigment-Protein Complexes

Antoine M. van Oijen,[1]* Martijn Ketelaars,[2] Jürgen Köhler,[1]† Thijs J. Aartsma,[2] Jan Schmidt[1]

Low-temperature single-molecule spectroscopic techniques were applied to a light-harvesting pigment-protein complex (LH2) from purple photosynthetic bacteria. The properties of the electronically excited states of the two circular assemblies (B800 and B850) of bacteriochlorophyll a (BChl a) pigment molecules in the individual complexes were revealed, without ensemble averaging. The results show that the excited states of the B800 ring of pigments are mainly localized on individual BChl a molecules. In contrast, the absorption of a photon by the B850 ring can be consistently described in terms of an excitation that is completely delocalized over the ring. This property may contribute to the high efficiency of energy transfer in these photosynthetic complexes.

The primary process in bacterial photosynthesis is the absorption of a photon by the light-harvesting antenna system, followed by the rapid and efficient transfer to the reaction center where the charge separation takes place. Typically, photosynthetic purple bacteria contain two types of antenna complexes, light-harvesting complexes 1 and 2 (LH1 and LH2, respectively), both of which are integral membrane proteins. The reaction center is presumed to be surrounded by the LH1 complex, whereas the LH2 complexes are arranged around the perimeter of the LH1 ring in a two-dimensional structure (*1*). The structure of the LH2 complex of the purple bacterium *Rhodopseudomonas acidophila* is known in great detail from x-ray crystallography (*2*), which has shown that the LH2 complex comprises 27 BChl a and (presumably) 18 carotenoid molecules noncovalently bound to the protein matrix. The BChl a molecules are organized in two concentric rings (Fig. 1). One ring, referred to as B800, features a group of nine well-separated BChl a molecules with an absorption band at ~800 nm. The other ring, referred to as B850, consists of 18 closely interacting BChl a molecules with an absorption band at ~860 nm. The entire LH2 complex is cylindrically symmetric with a ninefold symmetry axis. Upon excitation, energy transfer occurs from B800 to B850 molecules on a picosecond time scale (*3–5*), whereas among the B850 molecules, it is an order of magnitude faster (*6–8*). The transfer of energy from LH2 to LH1 and subsequently to the reaction center occurs in vivo on a time scale of 5 to 25 ps (*9*), very fast in comparison to the decay of B850 in isolated LH2, which corresponds to a lifetime of 1.1 ns.

Despite the fact that the LH2 complex has been intensively investigated in recent years with a wide variety of spectroscopic tools, including the observation of the fluorescence dynamics of single LH2 complexes (*10*), no clear picture of the electronic structure of its excited states exists. Here, we present the results of a study of isolated single LH2 complexes by single-molecule fluorescence-excitation spectroscopy, a method successfully applied in recent years to the detection of single guest molecules in crystalline and amorphous matrices (*11*). This technique allows the observation of optical spectra of individual complexes devoid of the ensemble averaging over static intercomplex disorder, thus directly revealing the salient properties of the electronic structure of the excited states.

The LH2 complexes of *R. acidophila* were prepared as described elsewhere (*3*). Hydrolyzed poly(vinyl alcohol) (PVA) with a weight-average molecular weight of 125,000 (obtained from British Drug House) was purified over a

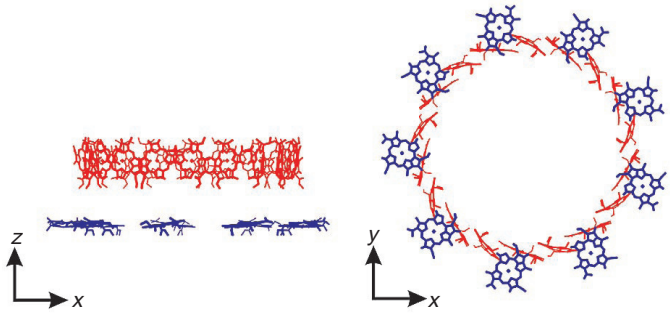

Fig. 1. Geometrical arrangement of the 27 BChl a molecules of the LH2 complex of *R. acidophila* obtained by x-ray crystallography. The B800 BChl a molecules are depicted in blue, and the B850 pigments are red. The phytol chains of the BChl a molecules are omitted for clarity. The data have been taken from the Protein Data Bank (identification code: 1kzu).

[1]Centre for the Study of Excited States of Molecules, [2]Department of Biophysics, Huygens Laboratory, Leiden University, Post Office Box 9504, 2300 RA Leiden, Netherlands.

*To whom correspondence should be addressed. E-mail: antoine@molphys.leidenuniv.nl

†Present address: Ludwig-Maximilians-Universität München, Sektion Physik und Center for NanoScience, Lehrstuhl für Photonik und Optoelektronik, Amalienstrasse 54, 80799 München, Germany.

mixed resin in order to remove ionic impurities. Thin polymer films, with a thickness of <1 μm, were prepared by adding 1% w/w purified PVA to a solution of 5×10^{-11} M LH2 in buffer (0.1% lauryldimethylamine *N*-oxide, 10 mM tris, and 1 mM EDTA, with pH 8.0), which was then spin coated on a LiF substrate (*12*). The samples were mounted in a cryostat, cooled to 1.2 K, and illuminated with a tunable continuous wave Ti-sapphire laser (spectral bandwidth of 1 cm^{-1}). Microscopic images could be obtained by wide-field illumination of the sample and imaging of the fluorescence at 890 nm on a charge-coupled device camera. Fluorescence-excitation spectra were then acquired by confocally exciting a spatially well-isolated complex and detecting its fluorescence (also at 890 nm) with an avalanche photodiode. In both cases, the detection bandwidth was 20 nm. More details can be found in (*13*).

In Fig. 2, the fluorescence-excitation spectra of several single LH2 complexes and an ensemble of LH2 complexes are compared. The ensemble spectrum features two broad structureless bands at ~800 and 860 nm, corresponding to the absorptions of the B800 and B850 pigments, respectively. When observing the single complexes, the ensemble averaging in these bands is removed, and remarkable spectral features become visible. The striking differences between the two absorption bands can be rationalized by considering the intermolecular interaction strength J between neighboring BChl a molecules in a ring and the spread in transition energies Δ. J is mainly determined by the intermolecular distance and the relative orientation of the molecular dipole moments. Variations in site energies Δ can often be attributed to structural variations in the environment of the BChl a molecules, resulting in changes in the electrostatic interaction with the surrounding protein. If the ratio J/Δ is small, it is expected that the excitations are mainly localized on individual BChl a molecules. If the coupling strength J between the BChl a molecules is much larger than Δ, the description should be in terms of delocalized excited-state wave functions with relatively short energy relaxation times.

As can be seen in Fig. 2, the B800 band of an individual LH2 complex consists of several relatively narrow spectral lines. From the width of the B800 ensemble line, a value of ~125 cm^{-1} for the diagonal disorder Δ can be extracted, and from the x-ray structure, it can be calculated, with a point-dipole approximation, that the interaction energy J between neighboring pigments amounts to -24 cm^{-1} (*14*). The ratio $|J/\Delta| \approx 0.2$ is characteristic for electronically excited states, which are largely localized on individual pigments. Therefore, the narrow lines around 800 nm can be attributed to the absorptions of individual BChl a molecules in the B800 ring. This interpretation is corroborated by the strong dependence of the relative intensities of these lines on the polarization of the incident radiation, consistent with the different directions of the dipole moments of localized transitions of BChl a molecules in the ring (*15*).

In the B850 band, the interaction strength between the BChl a molecules is determined to be ~300 cm^{-1} (*14*), that is, considerably larger than the disorder (estimated to be ~125 cm^{-1}). Therefore, we have to consider excitonic interactions in order to understand the optical spectra. As a starting point, we calculated the excited-state manifold of a cylindrically symmetric B850 assembly with zero disorder. Of the two nondegenerate (denoted as $k = 0$ and $k = 9$) and eight pairwise degenerate ($k = \pm1$, $k = \pm2$, . . ., $k = \pm8$) exciton states, only the low-energy degenerate pair $k = \pm1$ will carry appreciable oscillator strength (Fig. 3A, left). Upon introducing diagonal disorder in the ring, the pairwise degeneracies will be lifted, and the oscillator strength is redistributed over adjacent exciton states (*16*) (Fig. 3A, right). The transition dipole moments associated with the $k = \pm1$ transitions will have orthogonal polarizations. This orthogonality is maintained when disorder is introduced, assuming that the diagonal disorder is dominated by variations in electrostatic interactions and possibly intermolecular distances, rather than by changes in the orientations of the BChl a molecules.

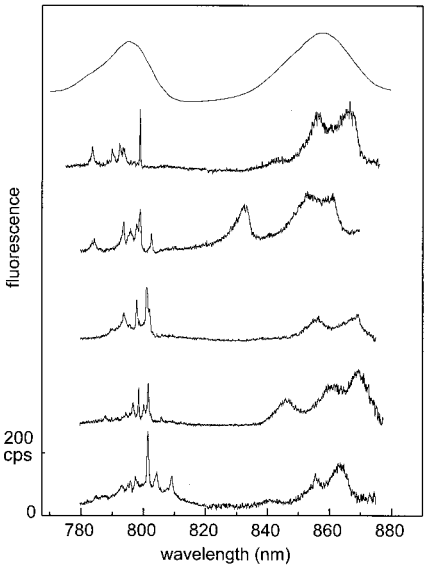

Fig. 2. Comparison of fluorescence-excitation spectra for an ensemble of LH2 complexes (top trace) and several individual LH2 complexes at 1.2 K. The vertical scale applies to the bottom spectrum; all other spectra are offset for clarity. cps, counts per second.

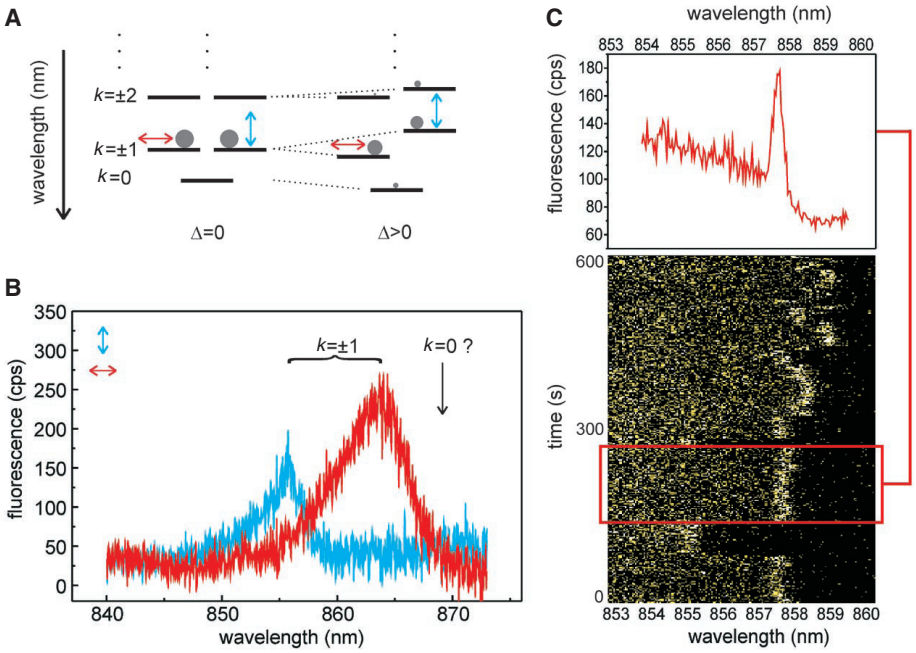

Fig. 3. (**A**) Schematic representation of the energy-level scheme of the lowest states in the excited-state manifold of the B850 ring in LH2 of *R. acidophila*. Compared are the relative positions of the lowest levels in the presence (left) and in the absence (right) of ninefold rotational symmetry. The gray circles indicate the initial population of a given excited state, and the arrows indicate the relative orientation of the transition dipole moments in the plane of the ring. (**B**) Fluorescence-excitation spectrum of the long-wavelength region of an individual LH2 complex for mutually orthogonal polarized excitation as schematically indicated in (A) by the colored arrows. (**C**) Fluorescence-excitation spectrum of the red wing of the long-wavelength absorption in the B850 band. In the bottom panel, a stack of 200 consecutively recorded spectra (3 s per scan) is shown where the fluorescence intensity is given by the color code (yellow corresponds to high intensities). The spectrum in the top panel corresponds to an average of only those scans that are covered by the box. For this particular complex, the whole set of lines in the B850 band is shifted toward higher energies in comparison to the complex shown in (B).

In all spectra of the single LH2 complexes we observed, the B850 band consisted of two broad absorption lines at ~860 nm, sometimes accompanied by a weaker third transition at the higher energy side. These observations can be explained in terms of the exciton model. The two absorptions correspond to the $k = \pm 1$ transitions, with their degeneracy lifted. By performing polarization-dependent experiments on these two bands (*17*), the orthogonality of the associated transition dipole moments, predicted by the exciton model, could be ascertained (Fig. 3B). This orthogonality was observed in all individual LH2 complexes that we studied and is a strong indication for a high degree of delocalization of the excitation. The observed homogeneous linewidth of the $k = \pm 1$ transitions of ~50 cm^{-1} is consistent with anisotropy decay times of ~100 fs found in pump-probe experiments (*8*). The extent of delocalization will decrease, and the dynamical properties will change at a higher temperature, where mixing of the exciton states by vibronic coupling will occur (*18*).

Another observation supporting the excitonic level scheme is the detection of the lowest exciton state $k = 0$. By repeatedly scanning the excitation wavelength quickly through the low-energy side of the $k = \pm 1$ pair and following the spectral features through time, the presence of the spectrally rapidly diffusing lowest exciton state could be made visible in a fraction (~25%) of the studied complexes (Fig. 3C). The low intensity of the $k = 0$ transition, which in principle is dipole forbidden, and spectral diffusion on a time scale faster than that of the experiment explain the absence of this lowest exciton transition in most of the complexes. The linewidth of the $k = 0$ state should be ~0.005 cm^{-1}, as determined by the 1.1-ns fluorescence lifetime of the system, but the observed value of ~5 cm^{-1} is mainly determined by residual spectral diffusion and the bandwidth of the excitation source.

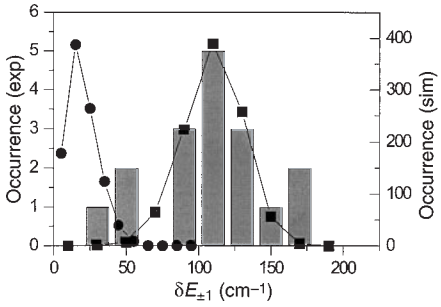

Fig. 4. The distribution of the energy separations $\delta E_{\pm 1}$ of the $k = \pm 1$ transitions. The histogram represents the experimental data (exp) for all complexes studied. The values obtained by numerical calculations (*19*), assuming only a disorder of 125 cm^{-1}, are depicted by solid black circles. After an additional elliptic deformation, with an eccentricity of $\varepsilon = 0.52$, is introduced in the simulations (sim), one obtains the data represented by solid black squares.

The energy splitting $\delta E_{\pm 1}$ between the $k = +1$ and $k = -1$ states was measured for all complexes investigated (Fig. 4). As mentioned previously, the presence of the disorder Δ forms a plausible cause for the lifting of the degeneracy of these exciton states. However, simulations show that the observed average $\delta E_{\pm 1}$ of ~110 cm^{-1} cannot be explained by taking into account only random disorder (as depicted in Fig. 4) for a simulated Δ with a full width at half-maximum (FWHM) of 125 cm^{-1} (*19*). Even an unreasonably large value of $\Delta \approx 500$ cm^{-1} for the width of the distribution of site energies did not result in an energy separation between the $k = \pm 1$ exciton states, as observed experimentally. To exclude the possibility that these abnormally high splittings are caused by an anisotropic environment in the polymer matrix, we repeated the experiment on single LH2 complexes in a glycerol matrix, which resulted in similar values of $\delta E_{\pm 1}$. A Jahn-Teller–like deformation in the excited state can probably be ruled out in view of the unrealistically high values needed for the electronic-nuclear coupling strength.

Although random disorder can give rise to large variations in the absorption wavelengths of the B850 bands (Fig. 2), the observed energy separation of the $k = \pm 1$ states can only be explained in terms of largely correlated disorder, such as a static symmetric distortion of the protein complex in the ground state. In the case of an elliptical deformation of the ring, it can be shown, on the basis of symmetry arguments, that only the $k = \pm 1$ exciton states will be split. This is consistent with the absence in the spectra of a splitting and a polarization effect of the $k = \pm 2$ states. The eigenfunctions of the $k = \pm 1$ states belong to the long and short axes of the ellipse and hence exhibit orthogonal polarization of their transition moments, as observed experimentally. Our simulations show that the observed splittings can be explained by assuming an eccentricity ε of the ring of 0.52, corresponding to a ratio of the long and short radius of 0.85, and a random disorder of 125 cm^{-1} (Fig. 4); $\varepsilon = (1 - a^2/b^2)^{1/2}$, where a and b are the length of the short and long axes, respectively. An explanation for the symmetry lowering in the LH2 from ninefold in the crystals used for resolving the x-ray structure to the twofold symmetry observed in our experiments may be found in the extremely dense packing of LH2 in the x-ray crystals, causing a stabilization of the structure. In our case of completely isolated complexes, these stabilizing forces are absent, and the complex deforms. What the symmetry properties of the LH2 are in a natural environment, surrounded by a limited number of LH2 complexes in the photosynthetic membrane, is therefore an intriguing question and deserves further study.

This work demonstrates that single-molecule spectroscopy is a powerful tool to reveal in detail the factors determining the electronic structure of pigment-protein complexes and, more generally, of molecular aggregates. Various manifestations of disorder can be probed directly, providing valuable information for the theoretical modeling of energy-transfer processes in these systems, a better understanding of the structure of these biologically important systems, and an understanding of how these systems function.

References and Notes

1. M. Z. Papiz *et al.*, *Trends Plant Sci.* **1**, 198 (1996).
2. G. McDermott *et al.*, *Nature* **374**, 517 (1995).
3. J. T. M. Kennis, A. M. Streltsov, H. Permentier, T. J. Aartsma, J. Amesz, *J. Phys. Chem. B* **101**, 8369 (1997).
4. R. Monshouwer, I. Ortiz de Zarate, F. van Mourik, R. van Grondelle, *Chem. Phys. Lett.* **246**, 341 (1995).
5. H.-M. Wu *et al.*, *J. Phys. Chem.* **100**, 12022 (1996).
6. M. Chachisvilis, O. Kühn, T. Pullerits, V. Sundström, *J. Phys. Chem. B* **101**, 7275 (1997).
7. R. Jimenez, S. R. Dikshit, S. E. Bradforth, G. R. Fleming, *J. Phys. Chem.* **100**, 6825 (1996).
8. S. I. E. Vulto, J. T. M. Kennis, A. M. Streltsov, J. Amesz, T. J. Aartsma, *J. Phys. Chem. B* **103**, 878 (1999).
9. V. Nagarajan and W. W. Parson, *Biochemistry* **36**, 2300 (1997).
10. M. A. Bopp, Y. Jia, L. Li, R. J. Cogdell, R. M. Hochstrasser, *Proc. Natl. Acad. Sci. U.S.A.* **94**, 10630 (1997).
11. Th. Basché, W. E. Moerner, M. Orrit, U. Wild, *Single Molecule Optical Detection, Imaging and Spectroscopy* (Verlag-Chemie, Munich, 1997).
12. LiF is a favorable substrate because the inversion symmetry of the alkali halide crystal prevents first-order Raman scattering.
13. A. M. van Oijen, M. Ketelaars, J. Köhler, T. J. Aartsma, J. Schmidt, *J. Phys. Chem. B* **102**, 9363 (1999).
14. K. Sauer *et al.*, *Photochem. Photobiol.* **64**, 564 (1996).
15. A. M. van Oijen, M. Ketelaars, J. Köhler, T. J. Aartsma, J. Schmidt, *Chem. Phys.*, in press.
16. R. G. Alden *et al.*, *J. Phys. Chem. B* **101**, 4667 (1997).
17. The polarization-dependent experiments were performed by rotating the polarization of the incident laser light in the plane of the sample. As a consequence of the high-velocity spin coating, the LH2 complexes are oriented predominantly flat on the substrate surface, perpendicular to the propagation vector of the excitation light. This was confirmed by similar experiments on LH2 complexes in non–spin-coated films.
18. J. A. Leegwater, *J. Phys. Chem.* **100**, 14403 (1996).
19. Monte Carlo simulations were performed on the basis of the crystal structure of LH2 of *R. acidophila*. Only nearest neighbor interactions were taken into account with the dipole-dipole approximation. A random diagonal disorder (FWHM = 125 cm^{-1}) was introduced for both the undistorted and distorted rings, assuming that it is centered at the same transition energy for every B850 pigment. In the case of the distorted ring, the individual pigments were positioned on an ellipse, whereas the long-wavelength (Q_y) transition dipoles retained the alignment as seen in the crystal structure.

20. The authors thank J. P. Abrahams (Leiden University, Leiden, Netherlands), J. Knoester (Groningen University, Groningen, Netherlands), and J. H. van der Waals (Leiden University, Leiden, Netherlands) for many helpful discussions. We also thank D. de Wit for the preparation of the LH2 complexes and M. Hesselberth for assistance with the spin coating. This work is supported by the Stichting voor Fundamenteel Onderzoek der Materie (FOM) with financial aid from the Nederlandse Organisatie voor Wetenschappelijk Onderzoek (NWO). J.K. is a Heisenberg fellow of the Deutsche Forschungsgemeinschaft.

8 April 1999; accepted 2 June 1999